



Thermal and Plasma-Enhanced ALD of Ta and Ti Oxide Thin Films from Alkylamide Precursors

W. J. Maeng and H. Kim^z

Department of Materials Science and Engineering, Pohang University of Science and Technology, Pohang 790-784, Korea

We investigated the thermal and plasma-enhanced atomic layer deposition (PE-ALD) of tantalum and titanium oxides from representative alkylamide precursors, Ta(NMe₂)₅ (pentakis(dimethylamino)Ta, PDMAT) and Ti(NMe₂)₄ [tetrakis(dimethylamido)Ti, TDMAT]. ALD of Ta₂O₅ by PDMAT with water or oxygen plasma produced pure Ta₂O₅ films with good self-saturation growth characteristics. However, incomplete self-saturation was observed for TiO₂ ALD from TDMAT. The film properties including microstructure, chemical composition, and electrical properties are discussed focusing on the comparative studies between thermal and PE-ALD processes for both oxides. The results indicate that the PDMAT is a promising precursor for both thermal and PE-ALD of Ta₂O₅.

© 2006 The Electrochemical Society. [DOI: 10.1149/1.2186427] All rights reserved.

Manuscript submitted December 27, 2005; revised manuscript received February 3, 2006.
Available electronically March 28, 2006.

Atomic layer deposition (ALD) is a gas-phase thin-film deposition method characterized by the alternate exposure of chemical species with self-limiting surface reactions, producing films with accurate thickness control, excellent conformality, and uniformity over large areas.¹ Due to these benefits, ALD is becoming one of the most promising thin-film deposition methods in the fabrication of nanoscale microelectronic devices, for which thickness controllability at atomic level and high conformality are required.² One of the critical issues for a successful ALD process is a proper selection of precursors and reactants. Among many metal precursors, alkylamide precursors have been widely used for ALD since they have suitable vapor pressure and Cl- and O-free ligands producing noncorrosive products and require relatively low growth temperatures.

ALD of high-*k* dielectrics have been extensively studied using a variety of precursors and reactants.³⁻⁶ As representative high *k* oxides, Ta₂O₅ and TiO₂ have been studied for various applications including capacitor and gate dielectrics for the semiconductor industry and chemical sensors.^{7,8} Although various precursors have been studied for ALD of Ta and Ti-based materials,^{4,9-12} alkylamide precursors have been widely used for deposition of TaN¹³ or TiN.¹⁴ For example, plasma-enhanced ALD (PE-ALD) of TaN from (pentakis(dimethylamino)Ta (PDMAT) and hydrogen plasma produced good quality TaN, showing very robust characteristics as a diffusion barrier for Cu interconnects.¹³ However, the alkylamide precursors have rarely been used for deposition of Ta or Ti oxide, except in a couple of very recent reports.^{15,16} This is quite contrary to other high-*k* materials such as ZrO₂ and HfO₂, for which extensive studies have been reported by thermal and PE-ALD from various alkylamide precursors.¹⁷⁻²⁰ Especially, no comparative study between thermal and PE-ALD from alkylamide precursors for Ta and Ti oxides has been reported yet. In this study, we investigated the thermal and PE-ALD processes of both oxides using representative alkylamide precursors, Ta(NMe₂)₅ [pentakis(dimethylamino)Ta, PDMAT] and Ti(NMe₂)₄ [tetrakis(dimethylamido)Ti, TDMAT], which have the same dimethylamino ligands. The film properties including microstructure, chemical composition, and electrical properties are discussed focusing on the comparative studies between thermal and PE-ALD processes for both oxides.

A homemade cold-wall-type remote PE-ALD chamber was built and used for this study. Sample sizes up to 200 mm in diameter can be loaded into the chamber pumped by a turbomolecular pump producing a working base pressure of middle 10⁻⁷ Torr. The sample was heated using a resistive heating plate, providing growth temperatures of up to 400°C. The temperature was measured using a thermocouple attached to the heater, and calibrated against another

thermocouple attached to the sample. The bubbler temperature containing PDMAT (solid) was set at 65°C to develop adequate vapor pressure while the delivery lines were heated to above 70°C to prevent condensation of the precursor. To improve gas delivery, Ar was used as a carrier gas and the flow was controlled by a mass-flow controller (MFC) upstream of the bubbler. For TDMAT, which has high enough vapor pressure, the bubbler remains at room temperature without the use of a carrier gas. For thermal ALD, the water vapor was used as a reactant. The bubbler containing water was immersed in silicone oil for better temperature control, and the water vapor flow was controlled by a leak valve. For PE-ALD, oxygen gas flowed into an rf plasma source, which consisted of a quartz tube wrapped with a multiple-turn coil set at 13.56 MHz providing a power level of up to 600 W. The distance between the remote plasma source and the sample during deposition is 20 cm. For the current experiments, the flow of oxygen, controlled by MFC, was set at 130 sccm, resulting in 10 mTorr of working pressure and the plasma power was 300 W. The chamber was purged by 75 sccm Ar gas between the precursor and reactant exposure step.

ALD oxide thin films were deposited on Si(001) substrates. For routine experiments, the substrates were cleaned by dipping in 1% HF solution for 1 min to remove the native oxide without a further cleaning process. However, the Si substrates for electrical property measurements were cleaned by the RCA method. After deposition, the thickness was routinely measured by ellipsometry (Rudolph auto ELII). The stoichiometry and impurity content in the thin films were analyzed by Rutherford backscattering (RBS) and X-ray photoemission spectroscopy (XPS). The microstructures of the films were determined by X-ray diffraction (XRD). For electrical measurements, a metal-oxide-semiconductor (MOS) capacitor structure was fabricated by evaporating 30 nm thick Al contact on 10 nm thick ALD oxide thin films through a shadow mask. For back contact, Au was evaporated on the back side and current-voltage characteristics were determined using HP4156 precision semiconductor parameter analyzer.

First, Ta₂O₅ thin films were deposited by thermal ALD from PDMAT and water vapor at a growth temperature of *T*_s = 250°C. The reactant (water) exposure time, *t*_r, was set as 3 s and the purging time, *t*_p, as 3 s. The growth rates, routinely measured by ellipsometry, are presented as a function of PDMAT exposure time, *t*_s, in Fig. 1. The growth rate increases rapidly with increasing *t*_s and saturates at ~0.85 Å/cycle at above *t*_s = 1 s. The saturation of the growth rate indicates that a typical ALD mode growth is achieved by self-limited adsorption of PDMAT. This growth rate was almost two times higher than the previously reported values from other precursors including ethoxide (0.45 Å/cycle) and chloride (0.45 Å/cycle).^{21,22} From the thickness vs growth cycles data (not shown), almost no nucleation delay was observed on Si(001).

^z E-mail: hyungjun@postech.ac.kr

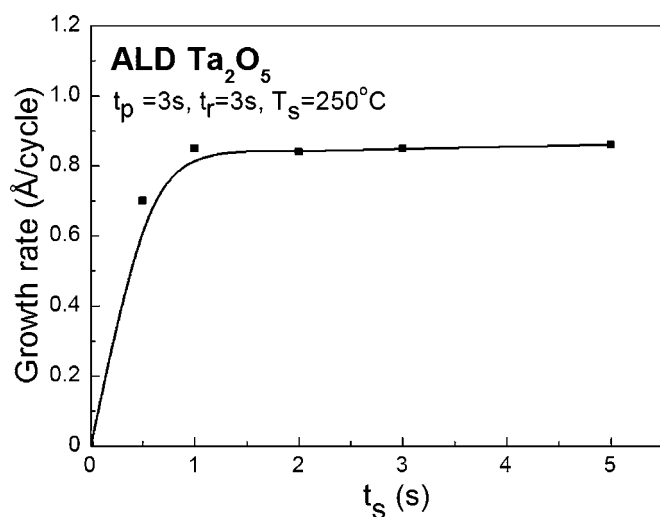


Figure 1. Growth rates of thermal ALD Ta_2O_5 as a function of PDMAT exposure time (t_s) on Si(001) substrate at $T_s = 250^\circ\text{C}$.

Next, Ta_2O_5 films were deposited by PE-ALD using O_2 plasma as a reactant and the growth characteristics were compared with those of thermal ALD. We did not perform detailed analysis on the reactive species of oxygen plasma. However, in a previous study on ALD ZrO_2 using a similar PE-ALD system, it was reported that the main species in the remote oxygen plasma are atomic oxygen and activated oxygen molecules by optical emission spectroscopy (OES).¹⁹ Figure 2 shows the growth rates as a function of reactant exposure time, t_r , at $T_s = 250^\circ\text{C}$ for both thermal and PE-ALD of Ta_2O_5 . The figure shows good saturation behavior at $t_r > \sim 1$ s for both cases, again indicating good saturation behavior of the PDMAT precursor. The growth rate of PE-ALD at saturation condition is about 1.2 Å/cycle, which is slightly higher than that of thermal ALD.

Figure 3 shows the growth rates of Ta_2O_5 thermal and PE-ALD at various growth temperature from $T_s = 100$ to 500°C with $t_s = 2$ s and $t_r = 3$ s. For both cases, three distinguished regions can be identified in the figure. In the middle temperature region, the growth rates remain almost constant, indicating the existence of a process window. For thermal ALD this region is from 200 to 250°C , while for PE-ALD it is from 150 to 250°C . In other words, the ALD can be achieved at almost 50°C lower temperature by PE-ALD than

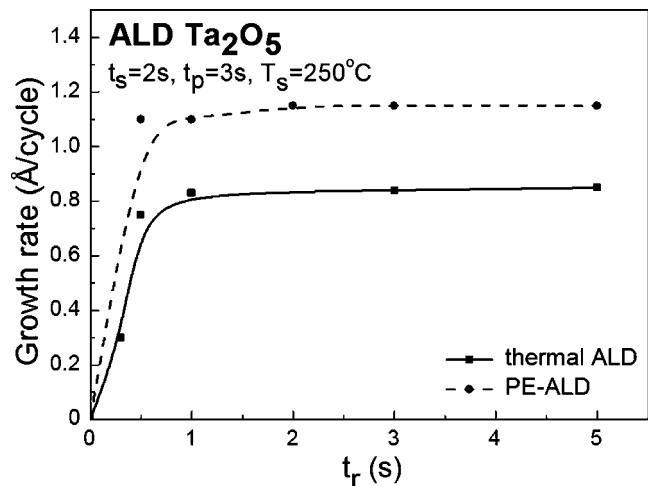


Figure 2. Growth rates of thermal and PE-ALD Ta_2O_5 as a function of water and oxygen plasma exposure time (t_r) on Si(001) substrate at $T_s = 250^\circ\text{C}$.

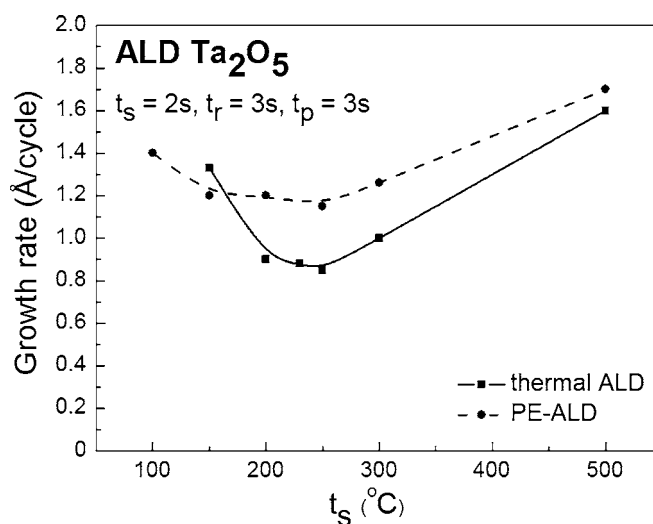


Figure 3. Growth rates of thermal and PE-ALD Ta_2O_5 as a function of growth temperature T_s .

by thermal ALD. This lower growth temperature is usually attributed to the higher reactivity of radicals, in this case atomic O or activated O_2 .²⁵ In fact, in a separate experiment, Ta_2O_5 film was not deposited without the use of plasma at $T_s \leq 250^\circ\text{C}$, indicating that the activated species generated by plasma are necessary to deposit Ta_2O_5 . In the high temperature region, the growth rates increase with increasing growth temperature. This behavior is due to the disturbance of self-limitation caused by thermal decomposition of precursors leading to partially CVD-like growth.² In the low growth temperature region, the growth rates increase with decreasing growth temperature for both thermal and PE-ALD. One of the plausible explanations proposed for this phenomenon is that the concentration of surface OH groups becomes higher with decreasing growth temperature, which leads to a larger number of active sites resulting in a higher growth rate in the low growth temperature region.^{24,25} This explanation could be generally applied for thermal ALD of oxide using water as a reactant. However, for PE-ALD using oxygen plasma as a reactant, the formation of an OH-terminated surface has not been clearly identified yet. In a more recent report, OES analysis of oxygen plasma indicated the presence of hydrogen radicals, which could result in OH-terminated surface by reaction of oxygen radicals with hydrogen likely to originate from precursors.²⁶ Thus, the same explanation would be applicable for PE-ALD of oxides, but more detailed experiments on the reaction mechanism of PE-ALD from oxygen plasma would be required to determine the exact reason for this behavior.

Next, TiO_2 films were deposited by thermal ALD from TDMAT and water. The growth rates as a function of TDMAT exposure time at $T_s = 200^\circ\text{C}$ are shown in Fig. 4. In contrast to Ta_2O_5 ALD from PDMAT, the growth rate did not saturate with increasing TDMAT exposure time, although some slow down of the growth rate at $t_s > 1$ s was observed. A possible explanation for this behavior is that the TDMAT molecules do not adsorb on the surface with perfect self-saturation, probably due to the low decomposition temperature of the TDMAT precursor, which is reported to be about 180°C .¹⁴ Similar behavior was reported for TiN ALD from TDMAT and NH_3 .¹⁴ However, we cannot exclude other possibilities for this non-ideal ALD growth, since the TiN ALD from TDMAT reported that the nonideal ALD mode was observed even at growth temperatures as low as 120°C . In any case, this nonideal ALD growth characteristic may limit the use of TDMAT as a precursor for TiO_2 ALD.

Based upon these results, the standard conditions were set as $t_s = 2$ s, $t_p = 5$ s, and $t_r = 3$ s for convenience sake. At this condition, the growth rate was about 2.1 Å/cycle, which was much higher than those from other previously reported precursors including

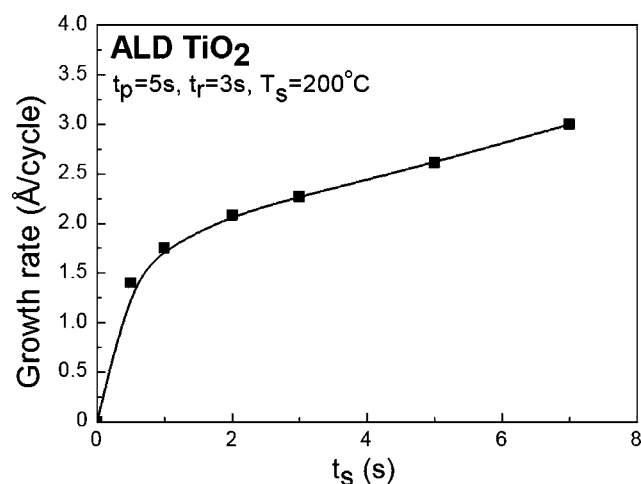


Figure 4. Growth rates of TiO_2 as a function of TDMAT exposure time on Si(001) substrate at $T_s = 200^\circ\text{C}$.

methoxide (0.5 \AA/cycle)⁴ and chloride (0.75 \AA/cycle).¹⁰ As a function of growth temperatures, similar growth characteristics as thermal ALD of Ta_2O_5 from PDMAT were observed for TiO_2 thermal ALD (data not shown). The growth rates of thermal ALD TiO_2 from TDMAT and water remained almost constant at $T_s = 150\text{--}250^\circ\text{C}$. PE-ALD of TiO_2 was also performed, and the typical growth rate was 2.17 \AA/cycle , which is slightly higher than that of thermal ALD.

The microstructures of thermal and PE-ALD Ta_2O_5 and TiO_2 films were analyzed by XRD. For thermal and PE-ALD Ta_2O_5 , the films were all amorphous in the growth temperature region studied ($150\text{--}350^\circ\text{C}$). For thermal ALD TiO_2 films, a however, a small anatase peak began to appear at $T_s = 250^\circ\text{C}$, and the intensity of the peak grew with an additional small rutile phase diffraction feature at $T_s = 300^\circ\text{C}$, while no diffraction peak was observed up to growth temperatures of 200°C . Similar results were reported for ALD TiO_2 from TiI_4 and H_2O_2 .¹¹ However, for an ALD of TiO_2 from $\text{Ti}(\text{OMe})_4$ and water, only anatase peaks were observed at $T_s > 250^\circ\text{C}$ without any rutile peak up to $T_s = 350^\circ\text{C}$,⁴ while no diffraction peak was observed for ALD TiO_2 thin film from $\text{Ti}(\text{O}^i\text{Pr})_2(\text{dmae})_2$ and water up to $T_s = 400^\circ\text{C}$.²⁷

Chemical compositions and binding states were analyzed by XPS for thermal and PE-ALD of Ta and Ti oxides. For both thermal and PE-ALD Ta_2O_5 , the only observed Ta-related XPS peaks were the standard Ta $4f_{7/2}$ peak (located at 26.5 eV) and Ta $4f_{5/2}$ peak (located at 28.4 eV) of Ta-O bond without any other Ta-related peaks such as Ta-N or metallic Ta. Besides, impurity-related peaks were not observed, indicating that the deposited Ta_2O_5 films are very pure (C, N $< 1\%$). Similarly, XPS results of TiO_2 thermal and PE-ALD have shown that the films are quite pure. For TiO_2 , however, a small nitrogen-related peak was observed, by which the nitrogen content was evaluated as $\sim 1.5\%$ for the samples grown at $T_s = 200^\circ\text{C}$. For more compositional information, RBS analysis was performed using oxygen, carbon, and nitrogen resonance. Agreeing with XPS analysis, no nitrogen or carbon-related feature were observed for Ta_2O_5 thin films.

As a representative electrical property of the deposited oxide films the leakage current density was estimated for thermal and PE-ALD of Ta_2O_5 and TiO_2 deposited at standard growth conditions on Si(001) substrate. Figure 5a and b present current density-electrical field plots for 10 nm thick, as-deposited Ta_2O_5 and TiO_2 ALD films, respectively. As Fig. 5a shows, the leakage current density of thermal ALD Ta_2O_5 film is $\sim 6 \times 10^{-5} \text{ A/cm}^2$ at 1 MV/cm . This value is comparable to that of CVD Ta_2O_5 using the same precursor and oxygen, which was grown at a much higher temperature, 450°C .²⁸

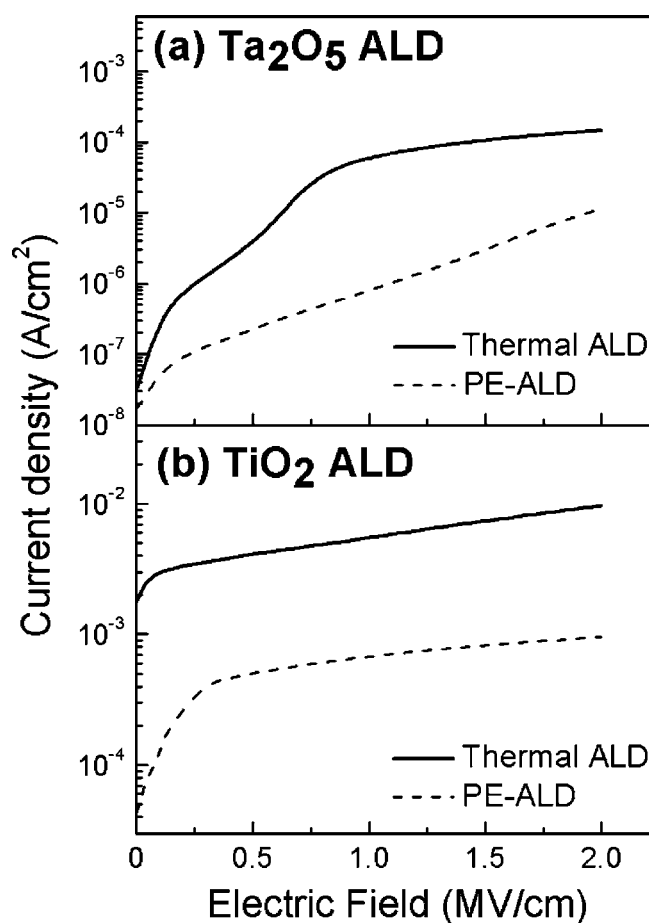


Figure 5. Leakage current densities vs electric fields of thermal and PE-ALD (a) Ta_2O_5 and (b) TiO_2 thin film. The film thickness was 10 nm for all films, and the growth temperatures were 250°C for Ta_2O_5 and 200°C for TiO_2 , respectively.

In a previous report, a lower leakage current density was reported for ALD Ta_2O_5 from PDMAT and water ($1 \mu\text{A/cm}$ for 10–100 nm thick films), but direct comparison with our result is difficult since the exact thickness and annealing conditions were not described.¹⁵ The leakage current density of our PE-ALD Ta_2O_5 is $\sim 8 \times 10^{-7} \text{ A/cm}^2$, which is about two orders of magnitude lower than that of thermal ALD. Also, this value is lower than that of previously reported PE-ALD Ta_2O_5 from ethoxide and oxygen plasma, $1 \times 10^{-6} \text{ A/cm}^2$ at 1 MV/cm for 15 nm thickness, indicating that high quality PE-ALD Ta_2O_5 films can be deposited from PDMAT and oxygen plasma.²⁹

Meanwhile, the leakage current densities of as-deposited TiO_2 thin films were $5 \times 10^{-3} \text{ A/cm}^2$ for thermal ALD and $7 \times 10^{-4} \text{ A/cm}^2$ for PE-ALD. A slightly higher leakage current density ($1 \times 10^{-3} \text{ A/cm}^2$ at 1 MV/cm) was reported for ozone-based ALD TiO_2 from the titanium isopropoxide precursor.³⁰ Moreover, a previous report using TDMAT and oxygen plasma produced TiO_2 films with a much higher leakage current density, larger than 1 A/cm for 1 MV/cm as-deposited sample.¹⁶

The results indicate that PE-ALD produced films with lower leakage current densities thermal ALD for both Ta_2O_5 and TiO_2 , even though the same metal precursor was used for each oxide. Similarly, it was reported that PE-ALD from zirconium *t*-but oxide produces of ZrO_2 films with two orders of magnitude lower leakage current density than thermal ALD.³¹ It was reported that defects such as an oxygen vacancy or C, Si contamination causes leakage currents in Ta_2O_5 films.³² Thus, a possible explanation for smaller leakage of PE-ALD oxides is smaller oxygen vacancy concentra-

tions or lower contamination (although the concentrations were below the detection limit in our experimental results) in PE-ALD films than in thermal ALD film. Additionally, smoother interface for PE-ALD than thermal ALD, observed by transmission electron microscopy (data not shown), might be partly responsible for this. However, further investigation will be necessary to clarify this.

In conclusion, tantalum and titanium oxide thin films were deposited by thermal and PE-ALD from PDMAT and TDMAT. The growth process was characterized as a function of various key growth parameters. For both cases, PE-ALD shows a higher growth rate at a lower growth temperature with better film quality. Pure Ta₂O₅ films were successfully deposited by thermal and PE-ALD from PDMAT with a good self-saturation property. Thus, PDMAT was found to be a promising precursor for both thermal and PE-ALD of Ta₂O₅, while TDMAT has shown nonideal growth with imperfect self-saturation behavior.

Acknowledgments

This work was supported by POSTECH, Korea Research Foundation, Korea Ministry of Industry and Energy. The authors are deeply thankful to Professor Shi Woo Rhee, Professor Wang Chul Zin, Professor Jong-Lam Lee, and co-workers at POSTECH for their contributions to this study. The RBS analysis was performed at Korea Institute of Science and Technology.

Pohang University of Science and Technology assisted in meeting the publication costs of this article.

References

1. M. Leskela and M. Ritala, *Angew. Chem., Int. Ed.*, **42**, 5548 (2003).
2. H. Kim, *J. Vac. Sci. Technol. B*, **21**, 2231 (2003).
3. J. Sundqvist, H. Hogberg, and A. Harsta, *Chem. Vap. Deposition*, **9**, 245 (2003).
4. V. Pore, A. Rathu, M. Leskela, M. Ritala, T. Sajavaara, and J. Keinonen, *Chem. Vap. Deposition*, **10**, 143 (2004).
5. J. Kim, S. Kim, H. Jeon, M. H. Cho, K. B. Chung, and C. Bae, *Appl. Phys. Lett.*, **87**, 053108 (2005).
6. H. Zhang, R. Solankia, B. Roberds, G. Bai, and I. Banerjee, *J. Appl. Phys.*, **87**, 1921 (2000).
7. K. W. Kwon, C. S. Kang, S. O. Park, H. K. Kang, and S. T. Ahn, *IEEE Trans. Electron Devices*, **43**, 919 (1996).
8. G. Eranna, B. C. Joshi, D. P. Runthala, and R. P. Gupta, *Crit. Rev. Solid State Mater. Sci.*, **29**, 111 (2004).
9. K. Kukli, M. Leskela, and M. Ritala, *Chem. Mater.*, **12**, 1914 (2000).
10. J. Aarik, A. Aidla, H. Mandara, T. Uustare, M. Schuisky, and A. Harsta, *J. Cryst. Growth*, **242**, 189 (2002).
11. K. Kukli, M. Ritala, M. Schuisky, M. Leskela, T. Sajavara, J. Keinonen, T. Uustare, and A. Harsta, *Chem. Vap. Deposition*, **6**, 303 (2000).
12. C. W. Hill, G. J. Derderian, and G. Sanju, *J. Electrochem. Soc.*, **152**, G386 (2005).
13. H. Kim, C. Detavenier, O. van der Straten, S. M. Rosnagel, A. J. Kellock, and D. G. Park, *J. Appl. Phys.*, **98**, 014308 (2005).
14. J. W. Elam, M. Schuisky, J. D. Ferguson, and S. M. George, *Thin Solid Films*, **436**, 145 (2003).
15. D. M. Hausmann, P. Rouffignac, A. Smith, R. Gordon, and D. Monsmab, *Thin Solid Films*, **443**, 1 (2003).
16. J. J. Park, W. J. Lee, G. H. Lee, I. S. Kim, B. C. Shin, and S. G. Yoon, *Integr. Ferroelectr.*, **68**, 129 (2004).
17. X. Liu, S. Ramanathan, A. Longdergan, A. Srivastava, E. Lee, T. E. Seidel, J. T. Barton, D. Pang, and R. G. Fordon, *J. Electrochem. Soc.*, **152**, G213 (2005).
18. A. Deshpande, R. Inman, G. Jursich, and C. Takoudis, *J. Vac. Sci. Technol. A*, **22**, 2035 (2004).
19. J. Y. Kim, S. H. Kim, H. Seo, J. H. Kim, and H. Jeon, *Electrochem. Solid-State Lett.*, **8**, G82 (2005).
20. S. J. Yun, J. W. Lim, and J. H. Lee, *Electrochem. Solid-State Lett.*, **7**, F81 (2004).
21. K. Kukli, M. Ritala, R. Matero, and M. Leskela, *J. Cryst. Growth*, **212**, 459 (2000).
22. J. C. Kwak, Y. H. Lee, and B. H. Choi, *Appl. Surf. Sci.*, **230**, 249 (2004).
23. K. E. Elers, J. Winkler, K. Weeks, and S. Marcus, *J. Electrochem. Soc.*, **152**, G589 (2005).
24. R. Puurunen, *Chem. Vap. Deposition*, **9**, 327 (2003).
25. J. Aarik, A. Aidla, V. Sammelselg, H. Siimon, and T. Uustare, *J. Cryst. Growth*, **169**, 496 (1996).
26. S. X. Lao, R. M. Martin, and J. P. Chang, *J. Vac. Sci. Technol. A*, **23**, 488 (2005).
27. J. P. Lee, M. H. Park, T. M. Chung, Y. S. Kim, and M. M. Sung, *Bull. Korean Chem. Soc.*, **25**, 475 (2004).
28. K. A. Son, A. Y. Mao, Y. M. Sun, B. Y. Kim, F. Liu, A. Kamath, J. M. White, D. L. Kwong, D. A. Roberts, and R. N. Vrtis, *Appl. Phys. Lett.*, **72**, 1187 (1998).
29. H. J. Song, C. S. Lee, and S. W. Kang, *Electrochem. Solid-State Lett.*, **4**, F13 (2001).
30. S. K. Kim, W. D. Kim, K. M. Kim, C. S. Hwang, and J. Jeong, *Appl. Phys. Lett.*, **85**, 4112 (2004).
31. K. Endo and T. Tatsumi, *Jpn. J. Appl. Phys., Part 2*, **42**, L685 (2003).
32. W. S. Lau, L. L. Leng, T. Han, and N. P. Sandler, *Appl. Phys. Lett.*, **83**, 2835 (2003).